

Path Tracking Controllers for Fast Skidding Rover

Mohamed Krid, Ziad Zamzami and Faiz Benamar

Abstract This article presents a comparative analysis between two new path tracking controllers, a linear and non-linear one. First, dynamic model of the vehicle moving on a horizontal plane is developed and validated with the experimental platform Spido. Then, to reduce the complexity, the model is linearized by assuming that the side slip angles remain small and a linear lateral slippage model introducing the lateral contact stiffness is used. The kinematics of the vehicle is also linearized by assuming that the rover remains close a reference path and with a small relative heading angle. The linearized model permits the design of a Linear Quadratic Regulator LQR that minimizing the angle deviation and the lateral error. Then, nonlinear predictive controller is presented. This approach combines the kinematic model of the path-tracking with the dynamic model of the vehicle to deduce a non-linear Continuous Generalized Predictive Controller NCGPC controller. The predictive approach is dedicated to achieve an accurate path tracking and minimizing the angle deviation and the lateral error during prediction horizon time. Finally, we compare performance results between the NCGPC and the LQR controller. The simulation results show that both controllers have equivalent path tracking performance only in the straight line sections. However, predictive controller clearly outperform LQR controller when cornering. NCGPC controller has a higher rate of convergence to the reference trajectory with minimal lateral position error, thanks to the anticipation of future reference path changes.

M. Krid

College of Engineering, Industrial Engineering, King Saud University,
Riyadh, Saudi Arabia
e-mail: mkrid@ksu.edu.sa

Z. Zamzami · F. Benamar (✉)

Institut des Systèmes Intelligents et Robotiques ISIR,
Sorbonne Universités, UPMC University, Paris 06, UMR 7222, 75005 Paris, France
e-mail: amar@isir.upmc.fr

Z. Zamzami

e-mail: zamzami@isir.upmc.fr

© Springer International Publishing Switzerland 2016

J. Filipe et al. (eds.), *Informatics in Control, Automation and Robotics 12th International Conference, ICINCO 2015 Colmar, France, July 21-23, 2015 Revised Selected Papers*,
Lecture Notes in Electrical Engineering 383, DOI 10.1007/978-3-319-31898-1_2

Keywords Mobile robot · Path tracking · Nonlinear continuous time generalized predictive control · LQR controller · Lateral slippage · Lateral dynamics

1 Introduction

Increasing adoption of outdoor mobile robots in challenging field conditions demand increasing capabilities in operating speed and distance range. Therefore we are interested in the design and control of fast rovers which are able to move autonomously in natural environment at high velocity (up to 10 m/s) following a reference path referred by RTK-GPS points. Generally, vehicle dynamics are neglected when designing the path tracking controller [1, 2], however purely kinematic based approaches are clearly incongruous for solving the problem of motion control of fast rovers.

Many researches focused on path following of autonomous vehicle in presence of sliding have been developed [1, 3]. This problem has an important nonlinearity in the dynamic and kinematic models. Usually a linearized model is used to resolve the control problems [4] and the vehicle dynamics are neglected. These approaches significantly reduce the control performance (accuracy, stability, robustness...).

On the other hand, when we observe animals or humans during their movement we understand that forward vision field is vital to anticipate the future state. Most of control laws do not explicitly take account the future state of the system and the implication of the current input on the future output (PID, LQR...) [5, 6]. This induces the idea of predictive control which depends not only on the actual state of the system but also on its predicted state. This capacity of fusion between actual dynamics, future predicted state and eventually constraints makes this control to be one of the most powerful [7]. In general, Model Predictive Control (MPC) uses linear models that makes model prediction solving sufficiently efficient to be runned in real time.

In off-road mobile robotics context and especially high speed, wheel's slippage and robot dynamics can not be neglected. Basic mobile robot control laws based on the ideal rolling assumption, as developed in [8] or [9], cannot be applied confidently. In order to improve the path tracking in presence of sideslip phenomena without reducing the robot speed, a nonlinear predictive approach will be used here and a closed-form control law will be defined.

In this paper, the approach of Nonlinear Continuous-time Generalized Predictive Control (NCGPC) is used for developing a robot path tracking controller and will be compared to the classical LQR approach. The model prediction considers the lateral dynamics, the wheel slippage and the nonlinear kinematics form of the path tracking problem. This article is organized as follow. We begins with a description of a 3-dof vehicle dynamic model, using a linear slippage model. The lateral dynamics model is then validated using the real robot. Afterward, the LQR approach is used in order to design a new controller for path tracking achievement. Finally, a non-linear model based predictive controller is then designed and generalized to

our multi-inputs multi-outputs dynamic system. Controller performances are then compared and validated using a Co-simulation ADAMS/Simulink model and the Spido experimental platform.

2 Lateral Dynamics Model

This section describes the vehicle dynamic model which will be used for control design. The model will be also discussed through experimental validation carried out on the Spido platform. This experimental platform is an off-road vehicle with four steered and driven wheels and with 4 independent suspensions shown in Fig. 1. The vehicle weight is about 620 kg and the front and rear half wheel base are respectively 0.62 m and 0.58 m. It is equipped with a Real Time Kinematic GPS (RTK-GPS) which supplies a localization with respect to a reference station accurate within ± 2 cm.

We consider in this section the double track model, well-known as the handling model, illustrated in Fig. 2. The vehicle model has 3 dof: longitudinal, lateral and yaw motions [10] of the chassis.

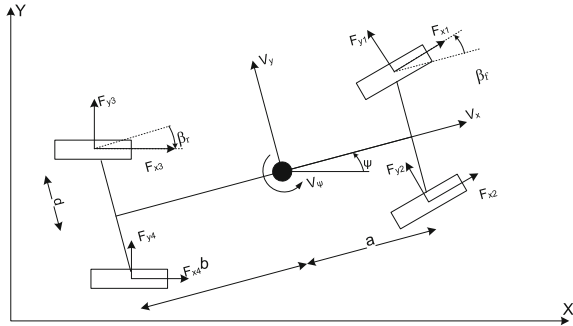
We denote by F_x and F_y the longitudinal and lateral tire forces, V_x and V_y the longitudinal and lateral velocities of the chassis center of mass, $\dot{\psi}$ is its yaw rate, I_z is the yaw-inertia moment, M is the car mass, d is the half-width of the wheel-base, a and b are the distances from the center of gravity to the front and rear axles and, β_f and β_r are front and rear wheel steering angles.

Except for the gravity and aero dynamic forces, the main external forces applied on the vehicle are produced by the tires. The lateral forces acting on the front and rear tire are assumed to be a linear function of the side-slip angle [11], i.e.

Fig. 1 The Spido experimental platform



Fig. 2 Model of the four-wheeled mobile robot



$$F_{y(f,r)} = C_{(f,r)} \alpha_{(f,r)} \quad (1)$$

where C_f and C_r are, respectively, the tire cornering stiffness of the front and rear tires.

The side-slip angle $\alpha_{f,r}$ is defined as the angle between the wheel velocity and the longitudinal axis of the wheel itself. Assuming that side-slip angles are quite small (less than 10° in practice), we can use a linear approximation, that is:

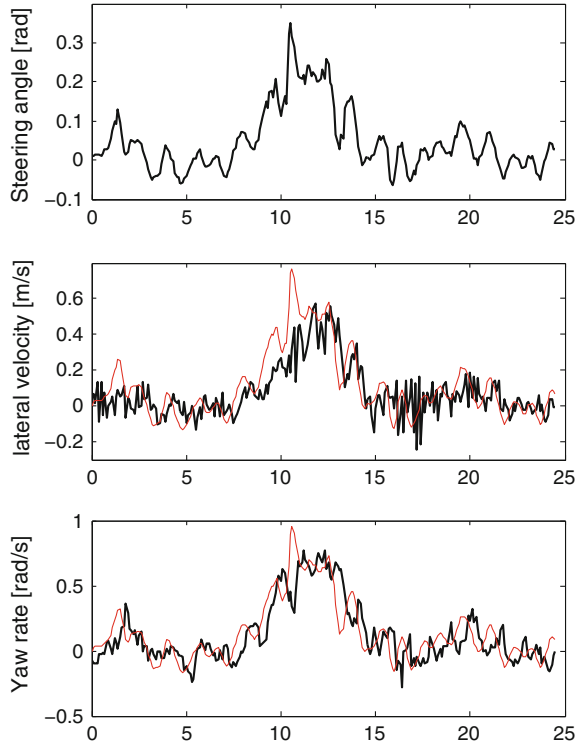
We focus in this paper on the lateral dynamics and the path tracking control. Henceforth, the longitudinal velocity V_x will be considered constant ($\dot{V}_x = 0$). The dynamic model can be then given by the following equation of motion.

$$\begin{pmatrix} \dot{V}_y \\ \dot{\psi} \end{pmatrix} = A \begin{pmatrix} V_y \\ \psi \end{pmatrix} + B \begin{pmatrix} \beta_f \\ \beta_r \end{pmatrix} + d \begin{pmatrix} 0 \\ \Delta F_{xf} + \Delta F_{xr} \end{pmatrix} \quad (2)$$

where ΔF_{xf} , ΔF_{xr} are front and rear traction force difference between right and left wheels, A and B are 2×2 matrix of:

$$\begin{aligned} a_{11} &= 2 \frac{C_f + C_r}{M V_x} & a_{12} &= 2 \frac{a C_f - b C_r}{M V_x} - V_x \\ b_{11} &= \frac{F_{xf} - 2 C_f}{M} & b_{12} &= \frac{F_{xr} - 2 C_r}{M} \\ a_{21} &= 2 \frac{a C_f - b C_r}{V_x I_z} & a_{22} &= 2 \frac{a^2 C_f + b^2 C_r}{V_x I_z} \\ b_{21} &= \frac{a(F_{xf} - 2 C_f)}{I_z} & b_{22} &= \frac{b(-F_{xr} + 2 C_r)}{I_z} \\ \alpha_f &= \frac{V_y + a \dot{\psi}}{V_x} - \beta_f, & \alpha_r &= \frac{V_y - b \dot{\psi}}{V_x} - \beta_r \end{aligned} \quad (3)$$

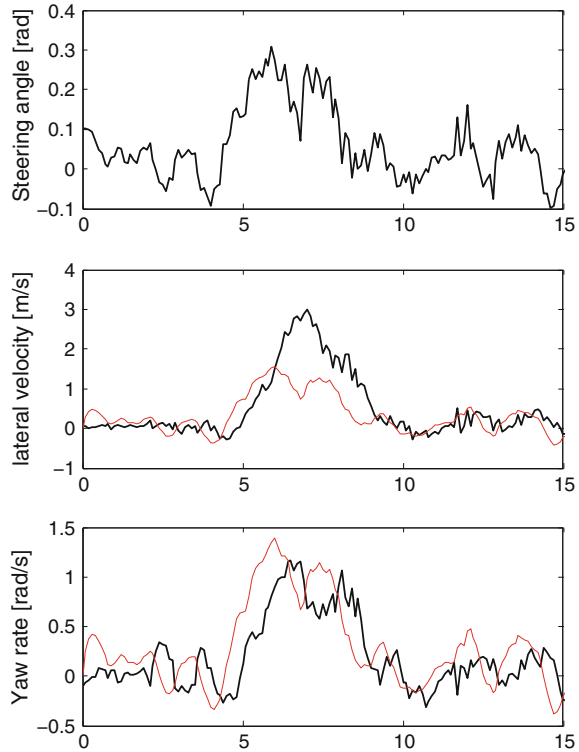
Fig. 3 Predicted (*red*) and measured (*black*) lateral velocity and yaw rate at 4 m/s



The linear state model described in (2) can be validated using the Spido platform.

The dynamic model described in (2) is identified and validated in an open loop controller. We compare from the real robot and the mathematical model output in Figs. 3 and 4 at different speeds, respectively 4 m/s and 6 m/s. In this validation stage, we consider the same trajectory for the different velocities. We assume constant all of the parameter of the state model matrix A and B except the longitudinal velocity V_x . We emphasize two observations in these tests: (1) the error between the measured and estimated lateral velocity varies with the magnitude of the velocity, as shown in Figs. 2, 3 and 4 we observe a clear delay between the measured and estimated value. These observations were key to enhance the performance of the controller as described in the following section.

Fig. 4 Predicted (*red*) and measured (*black*) lateral velocity and yaw rate at 6 m/s



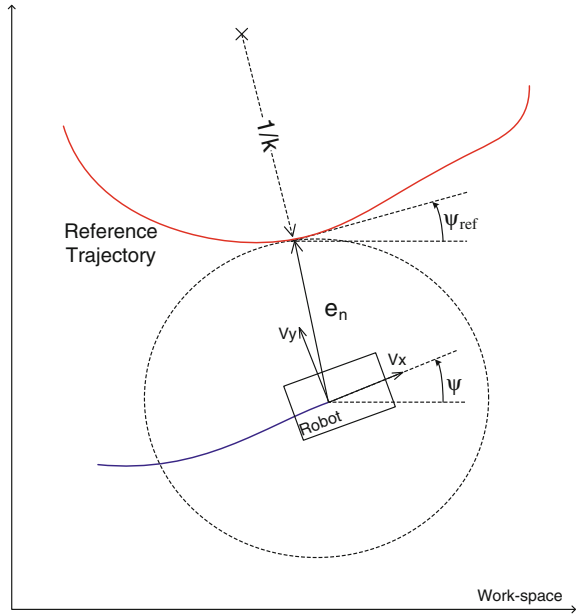
3 Linear Path Tracking Controller Design

3.1 Robot-Path Kinematic Model

We will consider in this section the design of a linear controller for tracking a given prescribed path defined in the horizontal plane and at a constant forward velocity ($\dot{V}_x = 0$). ψ and ψ_{ref} are the robot heading and the heading of the local tangent of the prescribed path with respect to a fixed arbitrary reference direction, as it can be illustrated in Fig. 5. The rate of change of ψ_{ref} with respect to the curvilinear distance measured along the path defines the path curvature k . e_ψ represents the heading error of the robot. e_n is the lateral deviation of the robot center of mass with respect to the prescribed path.

Sign conventions for both e_ψ and e_n are denoted in Fig. 5. With reference to the same figure and by assuming that the angular deviation is small, the following kinematical relationships are derived:

Fig. 5 The reference and actual path



$$\begin{aligned}\dot{e}_n &= V_x \sin e_\psi + V_y \cos e_\psi \\ &= V_x e_\psi + V_y\end{aligned}\quad (4)$$

$$\begin{aligned}\dot{e}_\psi &= \dot{\psi} - \dot{\psi}_{ref} \\ &= \dot{\psi} - \frac{V_x \cos e_\psi - V_y \sin e_\psi}{1/k + e_n}\end{aligned}\quad (5)$$

In case of straight line tracking ($k = 0$), this last equation is not singular and is equivalent to $\dot{e}_\psi = \dot{\psi}$, since $\dot{\psi}_{ref} = 0$ for a straight line path. Assuming that $e_n \ll 1/k$, Eq. (5) can be linearized as follow:

$$\dot{e}_\psi = \dot{\psi} - V_x k + V_x k^2 e_n \quad (6)$$

Assuming a constant curvature, the derivative with respect to time of this latter equation gives

$$\ddot{e}_\psi = \ddot{\psi} + V_x^2 k^2 e_\psi + V_x k^2 V_y \quad (7)$$

3.2 Design Control

In this section, we define a path tracking control of the robot using linear state feedback. Combing the kinematic model of the path-tracking errors (4) and (7) with the dynamic model of the vehicle (2) results in a new state-space model:

$$\dot{X} = AX + BU$$

where $X = [V_y \dot{\psi} e_\psi \dot{e}_\psi e_n]^T$ is the state vector and $U = [\beta_f \beta_r \Delta F_{xf} \Delta F_{xr}]^T$ is the inputs vector, A is 5×5 matrix and B is 5×4 matrix. In this study, the main objective of the control design is to improve the steering behavior of the robot in the presence of lateral and yaw disturbances. Therefore, the controller should minimizes the side-slip angle β of the robot center mass through minimizing lateral velocity V_y and its yaw rate (thereby decreasing the probability of lateral skidding). To achieve good tracking performance, the cost function must include a term that penalizes both the heading angle deviation e_ψ and the lateral offset e_n ,

$$J = \lim_{t \rightarrow \infty} \frac{1}{t} \int_0^t (X^T Q X + U^T R U) dt \quad (8)$$

The second term on the right-hand penalizes the weighted-magnitude of the control inputs vector. This will prevent the use of too high control commands and the resultant control actions will be smooth. Q and R are the nominal state-weighting and the input-weighting matrices.

3.3 Tracking Performance of the Linear Controller

In this section, the LQR controller presented in the previous section has been tested using co-simulation between ADAMS for the mechanical model and Matlab for the control one. The ADAMS model consider a mechanical model with 16 DOF, including 4 independent double wishbone suspensions. The classical Z and O paths are used for testing the controller, they are plotted respectively on (Figs. 6 and 10). In the simulation, the LQR controller gains are calculated on-line, as they depend on the longitudinal velocity V_x and the reference path curvature k . The path curvature was filtered to remove the abrupt variations. During the first 3 s of simulation, the system is open-loop until reaching the reference longitudinal velocity. For the first path, we give the control inputs for the front and rear steering angles. The time evolution of lateral deviation and orientation errors are shown on Figs. 8 and 9. For the second path, we give on Fig. 11 the differential forces ΔF_{xf} ΔF_{xr} for the front and the rear axles (Fig. 7).

Fig. 6 The reference (*blue*) and actual (*red*) paths for the 'Z' path

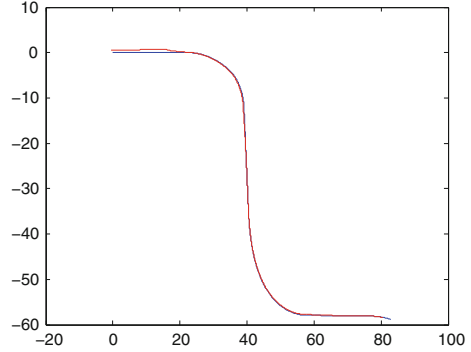


Fig. 7 Steering angles: front (*red*) and rear (*blue*) for the 'Z' path (rad)

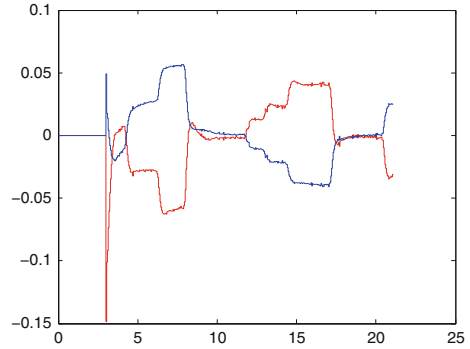
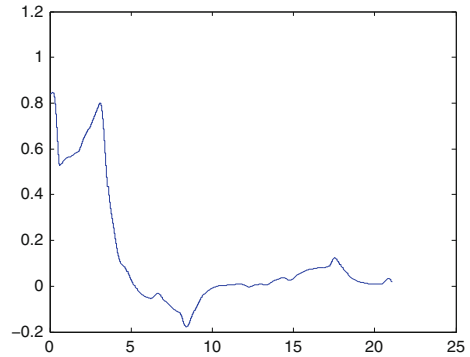


Fig. 8 Lateral deviation for the 'Z' path (m)



Results show that the proposed LQR control based on the dynamics model is able to track the reference path with quite good accuracy and quite small and smooth inputs. The new inputs controllers, ΔF_{xf} and ΔF_{xr} , seems to increase the rank of the controllability matrix what permits to reduce the steering angles.

Fig. 9 Yaw deviation for the ‘Z’ path (rad)

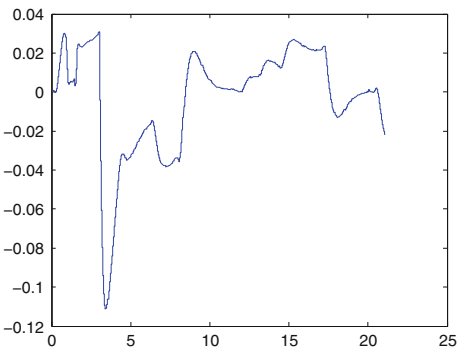


Fig. 10 The reference (*blue*) and actual (*red*) paths for the ‘O’ path

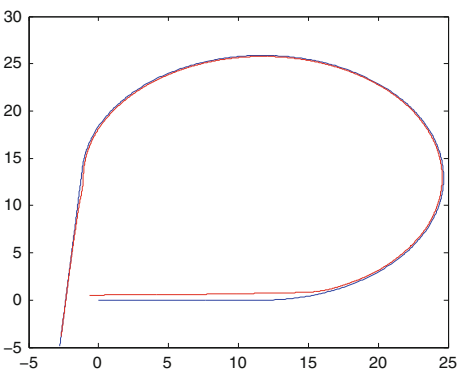
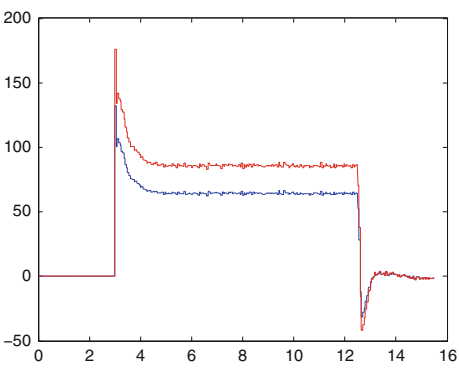


Fig. 11 The differential forces on front (*red*) and rear (*blue*) axle for ‘O’ path (N)



4 Nonlinear Predictive Approach

Using the dynamic model developed in the previous section, we will now define a predictive controller which have to minimize the tracking error along a receding time horizon. As with the linear approach, we assume a constant forward velocity ($\dot{V}_x = 0$). We combine the dynamic model of the vehicle (2) and the non-linear kinematic model of path tracking composed by the projection of the actual global position of the vehicle (X, Y) on the reference path. Using this model a nonlinear predictive control is computed, dedicated to achieve an accurate path tracking despite the nonlinear dynamical phenomena such as the bad grip conditions that leads to slipping.

Combing the dynamics model (2) and the kinematic one results in a new nonlinear state-space model:

$$\begin{aligned}\dot{V}_y &= a_{11}V_y + a_{12}V_\psi + b_{11}\beta_f + b_{12}\beta_r \\ \dot{V}_\psi &= a_{21}V_y + a_{22}V_\psi + b_{21}\beta_f + b_{22}\beta_r \\ \dot{\psi} &= V_\psi \\ \dot{X} &= V_x \cos \psi - V_y \sin \psi \\ \dot{Y} &= V_x \sin \psi + V_y \cos \psi\end{aligned}\tag{9}$$

We define the output y by:

$$y = \begin{pmatrix} \psi \\ X \\ Y \end{pmatrix}$$

Although a linear kinematic model is usually used [5] to simplify the controller form, in our case, we choose a nonlinear kinematic model for increased accuracy. The delay observed earlier when we compared the measured and estimated value of the state of the model (2) and the nonlinear form of the kinematic model motivate us to choose Nonlinear Continuous-time Generalized Predictive Control.

4.1 NCGPC Based Controller Design

To introduce the design of NCGPC controller, we can write the dynamic model (9) in the following form:

$$\begin{aligned}\dot{x} &= f(x) + g(x)u \\ y &= (h_1(x), \dots, h_m(x))\end{aligned}$$

where, the state vector $x \in \mathbb{R}^n$, the output $y \in \mathbb{R}^m$ and input $u \in \mathbb{R}^p$. The NCGPC controller minimizes a quadratic cost criterion which is based on the difference

between the predicted state y and a reference signal w . We denote $e_i(t)$ the error between the output h_i and the reference signal $w_i(t)$ at the time t and $w = (w_1(t) \dots w_m(t))$.

$$e_i(t) = h_i(x(t)) - w_i(t) \quad (10)$$

The output prediction is based on the expansion in Taylor series. An approximation of the reference signal is done in the same way.

$$\hat{y}(t + \tau) = \sum_{k=0}^{\rho} y^{(k)}(t) \frac{\tau^k}{k!} + R(\tau^\rho) \quad (11)$$

We can define the cost function as following

$$J_i = \frac{1}{2} \int_0^{T_i} [\hat{e}_i(t + \tau)]^2 d\tau \quad (12)$$

where T_i is the prediction horizon time of the i th output h_i and τ a given value belonging to the time interval $[t, t + T_i]$. We then deduce the global cost function J :

$$J = \sum_{i=1}^m J_i = \frac{1}{2} \sum_{i=1}^m \left(\int_0^{T_i} [\hat{e}_i(t + \tau)]^2 d\tau \right) \quad (13)$$

To derive the control law, we need to minimize the expression (13) of the criterion with respect to control u :

$$\frac{\partial J}{\partial u} = 0_{p \times 1} \quad (14)$$

The analytical expression of the control law u can be found in (14). The analytical expression of the control law is not detailed in this paper. To understand this issue, more information can be found in [12–14]. It was demonstrated that the stability of such NCGPC controller is guaranteed for system having a relative degree of each output less than or equal to four. That is particularly true for our system.

4.2 Simulation and Experimental Results

The NCGPC controller presented in the previous section has been tested using co-simulation between Adams for the plant model and Matlab/Simulink for the control one. The Adams model considers a multibody system with 16-dof, including 4 independent double wishbone suspensions. The wheel-ground contact model is the solid/solid native model composed by a series of non-linear spring-damper for

normal forces and a regularized Coulomb friction model for tangential forces. The slope at the origin of the latter will give contact stiffness C_f and C_r defined in Sect. 2.

The classical O -shaped paths are used for testing the controller. Since the simulation should start preferably from equilibrium, during the first 3 s of simulation, the vehicle is open-loop driven till it reaches the reference longitudinal velocity.

Figures 13 and 14 illustrate controller performance with initial error at two velocity levels $V_x = 4$ m/s and $V_x = 6$ m/s. Each one compares the actual and the reference paths in the horizontal plane. We can appreciate the effect of vehicle velocity during the transition phase between the straight line and the curvilinear sections; the controller's rate of convergence to the reference trajectory is inversely proportional to the robot's velocity. We denote that the simulation started with an initial lateral deviation of 1.2 m and we use a time receding horizon of 0.6 s. Furthermore, we can deduce from the position and angular error at $V_x = 4$ m/s in Figs. 15 and 16, respectively at $V_x = 6$ m/s in Figs. 17 and 18, that the NCGPC controller provides equivalent performance. We notice that the controller stabilizes the initial position error during

Fig. 12 CAD view of the used 16-dof Adams model

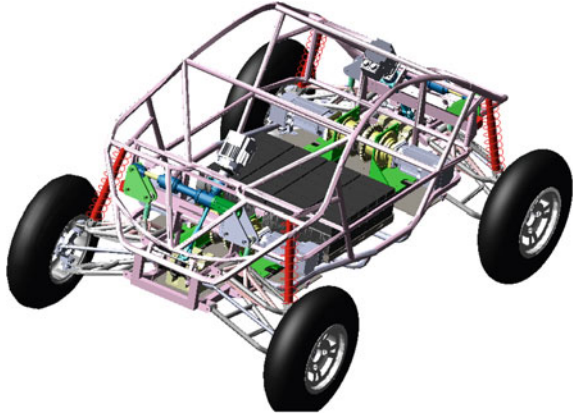


Fig. 13 Reference (red) and actual (blue) robot position (m) at $V_x = 4$ m/s

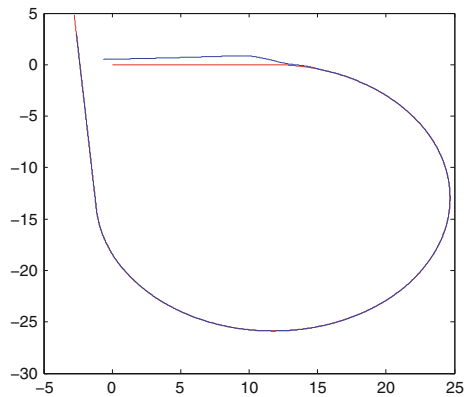


Fig. 14 Reference (*red*) and actual (*blue*) robot position (m) at $V_x = 6$ m/s

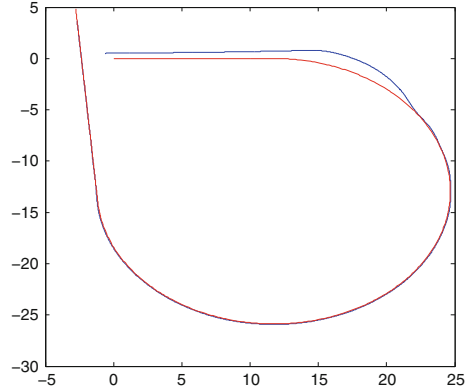


Fig. 15 Angular deviation (rad) versus time (s) graph at $V_x = 4$ m/s

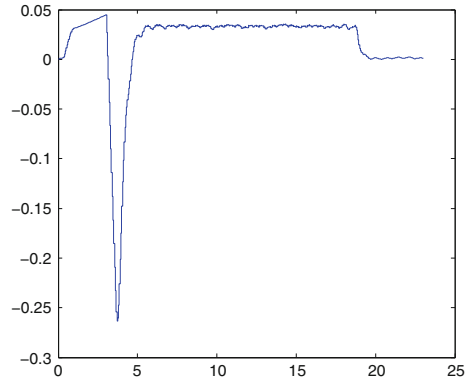
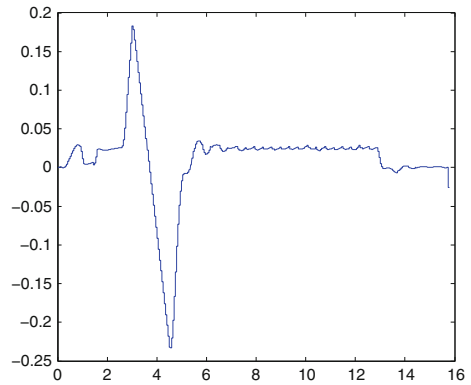


Fig. 16 Angular deviation (rad) versus time (s) graph at $V_x = 6$ m/s



the first second and start anticipation the path curvature change at approximately 1 s (Fig. 12).

We compare performance results of the *NCGPC* controller developed in this paper to the *LQR*-based controller developed in Sect. 3. Figure 19 shows the reference path

Fig. 17 Lateral deviation (m) versus time (s) graph at $V_x = 4$ m/s

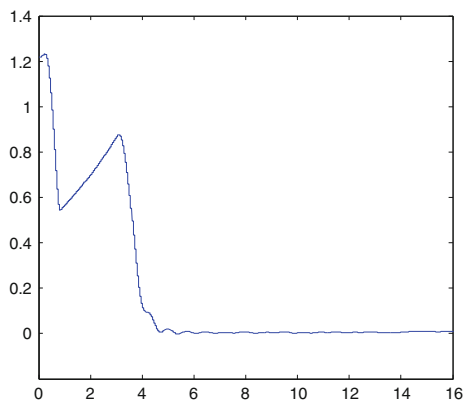


Fig. 18 Lateral deviation (m) versus time (s) graph at $V_x = 6$ m/s

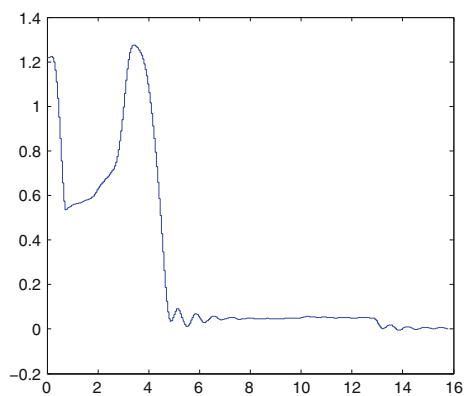
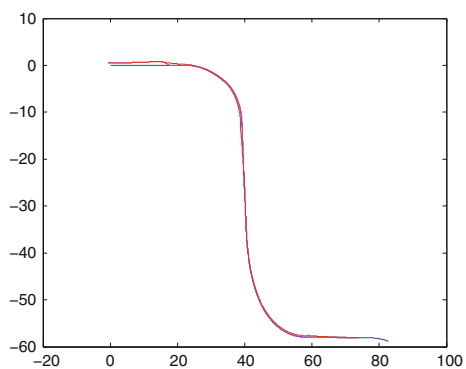


Fig. 19 Comparing 2 different controllers: LQR (red) versus NCGPC (magenta) robot position



in blue and the performed paths in red and magenta colors using the LQR and NCGPC controllers respectively. We can deduce that both controllers have equivalent path tracking performance only in the straight line sections. However, predictive controller clearly outperform LQR controller when cornering as shown in Fig. 22. NCGPC

Fig. 20 Steering angle (rad) versus time (s) graph: LQR (red) and NCGPC (blue)

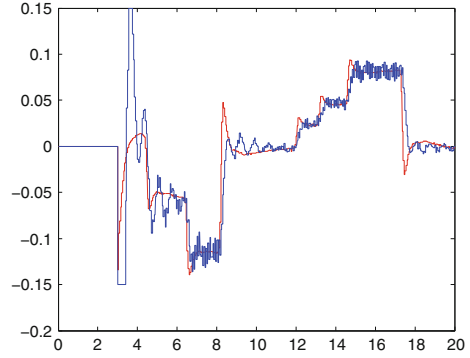


Fig. 21 Angular error (rad) versus time (s) graph: LQR (red) and NCGPC (blue)

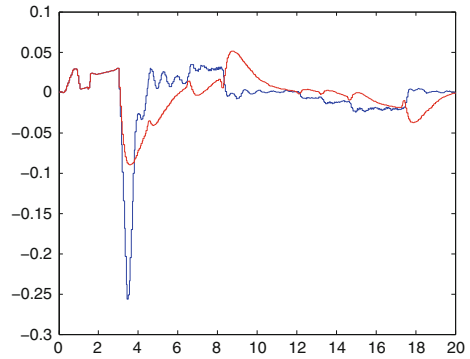
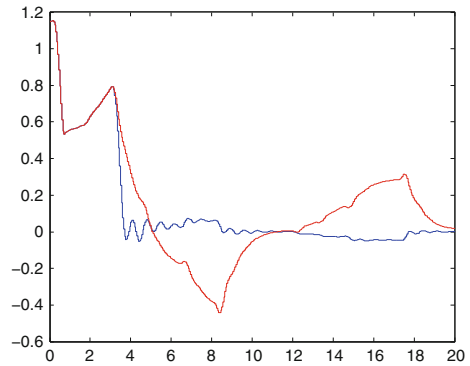
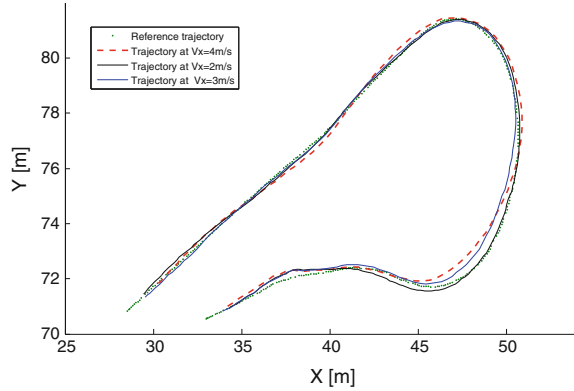


Fig. 22 Lateral deviation (m) versus time (s) graph: LQR (red) and NCGPC (blue)



controller has a higher rate of convergence to the reference trajectory with minimal lateral position error, thanks to the anticipation of future reference path changes. The predictive controller can track the path with a small lateral error comparing to the pure feedback-based LQR controller. It is clearly shown that this latter can not control accurately the lateral dynamics and the sideslip angle (Figs. 20 and 21).

Fig. 23 Experimental results: performed paths at different velocities using the predictive NCGPC controller



We observe that there is no difference between both controllers, during the straight line phase and at the end of the path when the robot reduces its velocity, this is mainly due to the low presence of the sideslip phenomena in these operating conditions (low steering angle and velocity).

The NCGPC controller presented has been also tested using the Spido experimental platform. The classical *O* paths (Fig. 23) was used for testing the controller at different forward velocities, $V_x = 2, 3, 4$ m/s. The path to be followed is recorded by a preliminary run achieved in manual driving. The testing conditions induced perturbations due to the terrain irregularities and friction conditions changes. The ground is composed by concrete area and wet nonuniform grass area where the vehicle is inevitably prone to slide. We must notice that our controller model is based on constant front and rear cornering stiffness. But thanks to controller robustness, the control law ensure a trajectory tracking with low tracking errors. The errors increase with velocities because of lateral slippage are increasing and probably roll angle as well which leads to stability limit and to the limitation of the model. We must note that the lateral acceleration reaches $0.7g$ which is the maximal value of the availability of the friction linear model and dynamic friction coefficient of 0.7 .

5 Conclusion

In this work, we present two controllers for mobile robot path tracking with high speed and dynamics. The mobile robot is a four wheel steered rover with suspension and capable to perform high speed cornering on natural ground. By combining the dynamic model of the vehicle, a slip based tyre model and a classical kinematic model of path tracking model, a linear and nonlinear model are deduced and validated using the real robot. Based on minimization of tracking error cost function along a receding time horizon, then nonlinear continuous-time generalized predictive control (NCGPC) has been designed and its performance is compared to that of the LQR

controller. Simulation and experimental results show a clear advantage of predictive controller when it comes to efficient and stable path tracking. This superiority is more pronounced for high speed motion and high curvature cornering, simply because such controller predict the robot behaviour over a receding time horizon and choose the optimal control input which drive the plant along the prescribed trajectory. An important advantage of the proposed solution is its easy integration because this controller supply an analytical expression of the control law u that reduce the real time calculation which simplify the implementation of the controller algorithm. This work will be continued to extend the NCGPC approach to redundant steering system, that includes front and rear steering and differential torque due to traction forces. Also, in order to increase the controller performance, another challenge for this study concerns the definition of the optimal prediction horizon time, probably as function of path curvature.

Acknowledgments This work was supported by the French ANR project EquipEx RobotEx (ANR-10-. EQPX-44).

References

1. Fang, H., Lenain, R., Thuilot, B., Martinet, P.: Trajectory tracking control of farm vehicles in presence of sliding. In: 2005 IEEE/RSJ International Conference on Intelligent Robots and Systems, 2005. (IROS 2005), pp. 58–63 (2005)
2. Tan, S.L., Gu, J.: Investigation of trajectory tracking control algorithms for autonomous mobile platforms: theory and simulation. In: 2005 IEEE International Conference Mechatronics and Automation, vol. 2, pp. 934–939 (2005)
3. Bouton, N., Lenain, R., Thuilot, B., Fauroux, J.-C.: A rollover indicator based on the prediction of the load transfer in presence of sliding: application to an all terrain vehicle. In: 2007 IEEE International Conference on Robotics and Automation, pp. 1158–163 (2007)
4. Yang, J.-M., Kim J.-H.: Sliding mode control for trajectory tracking of nonholonomic wheeled mobile robots. *IEEE Trans. Robot. Autom.* **15**(3), 578–587 (1999)
5. Krid, M., Ben Amar, F.: A dynamic based path tracking controller for a fast rover with independent steering and drive. In: International Conference on Climbing and Walking Robots and the Support Technologies for Mobile Machines, Sept 2011
6. Padhy, P.K., Majhi, S.: On-line mobile robot path tracking using PI controller. In: India Conference, 2006 Annual IEEE, pp. 1–4, Sept 2006
7. Rossiter, J.A.: Model Based Predictive Control: A Practical Approach, Control Series. CRC PRESS (2003)
8. Cariou, C., Lenain, R., Thuilot, B., Martinet, P.: Adaptive control of four-wheel-steering off-road mobile robots: application to path tracking and heading control in presence of sliding. In: IEEE/RSJ International Conference on Intelligent Robots and Systems, 2008. IROS 2008, pp. 1759–1764, Sept 2008
9. Micaelli, A., Samson, C.: Trajectory tracking for unicycle-type and two-steering-wheels mobile robots. Research report rr-2097, INRIA (1993)
10. Liaw, C.C., Chung, W.C., Song, C.C., Hsieh, C.-S.: A feedback linearization design for the control of vehicle's lateral dynamics. In: SICE-ICASE, 2006. International Joint Conference, pp. 4937–4942, Oct 2006
11. Jung, S., Hsia, T.C.: Explicit lateral force control of an autonomous mobile robot with slip. In: 2005 IEEE/RSJ International Conference on Intelligent Robots and Systems, 2005. (IROS 2005), pp. 388–393, Aug 2005

12. Chen, W.H.: Predictive control of general nonlinear systems using approximation. *IEE Proc. Control Theory Appl.* **151**(2), 137–144 (2004)
13. Gawthrop, P.J., Ballance, D.J., Chen, W.H.: Optimal control of nonlinear systems: a predictive control approach. *Automatica*, **39**(4), 633–641 (2003). Final version as accepted by Automatica supplied by the author
14. Dabo, M., Chafouk, H., Langlois, N.: Unconstrained NCGPC with a guaranteed closed-loop stability: case of nonlinear siso systems with the relative degree greater than four. In: *Proceedings of the 48th IEEE Conference on Decision and Control, 2009 held jointly with the 2009 28th Chinese Control Conference. CDC/CCC 2009*, pp. 1980–1985, Dec 2009

Informatics in Control, Automation and Robotics 12th
International Conference, ICINCO 2015 Colmar, France,
July 21-23, 2015 Revised Selected Papers

Filipe, J.; Madani, K.; Gusikhin, O.; Sasiadek, J. (Eds.)

2016, XVII, 412 p. 239 illus., 165 illus. in color.,

Hardcover

ISBN: 978-3-319-31896-7